Application Note AN-4150

Design Guidelines for Flyback Converters Using FSQ-series Fairchild Power Switch (FPS™)

1. Introduction

Compared to conventional hard-switched converters with fixed switching frequencies, the quasi-resonant converter (QRC) topology is a very attractive alternative for power supply designers. The increasing popularity of the QRC approach is based on its ability to reduce electromagnetic interference (EMI) while increasing power conversion efficiency.

The FSQ-series FPS™ (Fairchild Power Switch) is an integrated Pulse Width Modulation (PWM) controller and Sense FET specifically designed for quasi-resonant off-line Switch Mode Power Supplies (SMPS) with minimal external components. Figure 1 shows the internal block diagram of the FSQ-series. Compared with discrete MOSFET and PWM controller solution, it can reduce total cost, component count,

size and weight, while simultaneously increasing efficiency, productivity, and system reliability. The FSQ-series employs an advanced control technique that allows converter to operate with narrow frequency variation, while keeping the quasi-resonant operation. When the converter operates in discontinuous conduction mode (DCM), the controller finds the valley of the drain voltage and turns on the MOSFET at the minimum drain voltage. Meanwhile, the converter can operate with fixed frequency when operating in continuous conduction mode (CCM), which allows converter design as simple as conventional PWM converters.

This application note presents practical design considerations of a flyback converter employing the FSQ-series FPS™. It covers designing the transformer, output filter, and sync network; selecting the components; and closing the feedback loop.
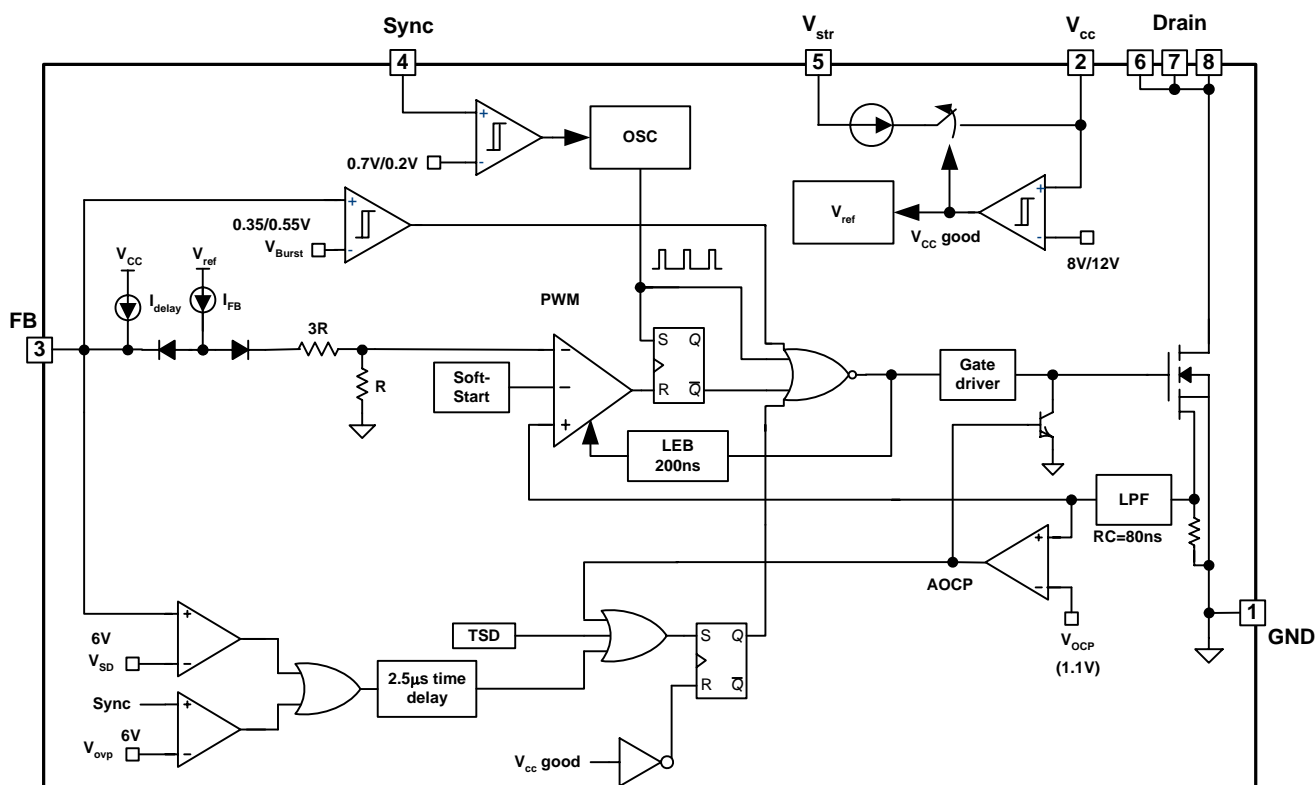

Figure 1. Block Diagram of FSQ-Series

2. Operation principle of Quasi-resonant flyback converter

Quasi resonant flyback converter topology can be derived from a conventional square wave, pulse-width-modulated (PWM) flyback converter without adding additional components. Figure 2 shows the simplified circuit diagram of a quasi-resonant flyback converter and its typical waveforms. The basic operation principles are:

■ During the MOSFET ON time (t_{ON}), input voltage (V_{IN}) is applied across the primary-side inductor (L_m). Then, MOSFET current (I_{ds}) increases linearly from zero to the peak value (I_{pk}). During this time, the energy is drawn from the input and stored in the inductor as much as $L_m \times I_{pk}^2/2$.

■ When the MOSFET is turned off, the energy stored in the inductor forces the rectifier diode (D) to turn on. During the diode ON time (t_D), the output voltage (V_o) is applied across the secondary-side inductor and the diode current (I_D) decreases linearly from the peak value ($I_{pk} \times N_p/N_s$) to zero. At the end of t_D, all the energy stored in the inductor has been delivered to the output. During this period, the output voltage is reflected to the primary side as $V_o \times N_p/N_s$. The sum of input voltage (V_{IN}) and the reflected output voltage ($V_o \times N_p/N_s$) is imposed on the MOSFET.

■ When the diode current reaches zero, the drain-to-source voltage (V_{ds}) begins to oscillate by the resonance between the primary-side inductor (L_m) and the MOSFET output capacitor (C_{oss}) with an amplitude of $V_o \times N_p/N_s$ on the offset of V_{IN}, as depicted in Figure 2. Quasi-resonant switching is achieved by turning on the MOSFET when V_{ds} reaches its minimum value. Doing this reduces the MOSFET turn-on switching loss caused by the capacitance loading between the drain and source of MOSFET. If the transformer is designed so that the resonance amplitude is larger than V_{IN} by increasing the turns ratio, N_p/N_s, "Zero-Voltage-Switching (ZVS)" of the MOSFET is achieved.

Other than turning on the MOSFET with minimum drain-to-source voltage, a quasi-resonant converter provides "soft" switching conditions to the switching devices. The MOSFET turns on at zero current and the diode turns off at zero current. This soft switching not only reduces the switching losses, but also lowers the switching noise caused by diode reverse recovery.

The major drawback of applying a quasi-resonant converter topology is that it causes the switching frequency to increase as the load decreases and/or input voltage increases. As the load decreases and/or input voltage increases, the MOSFET ON time (t_{ON}) diminishes and, therefore, the switching frequency increases. This results in severe switching losses, as well as intermittent switching and audible noise. Due to these problems, the conventional quasi-resonant converter topology has limitations for applications with wide input and load ranges.
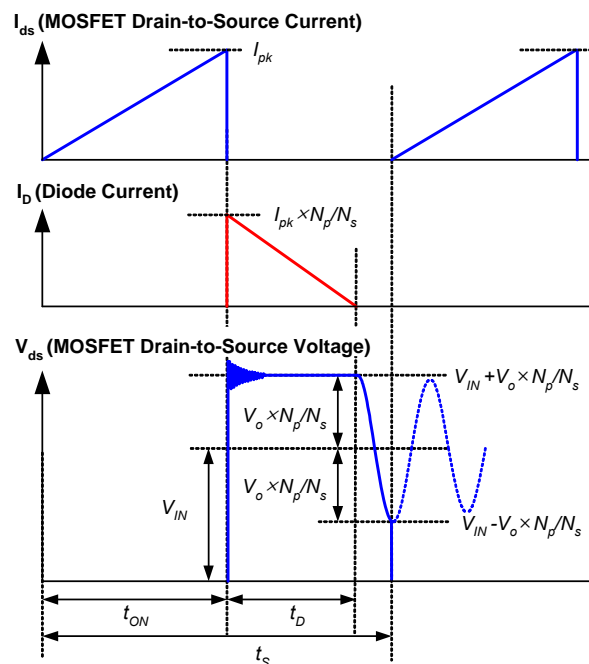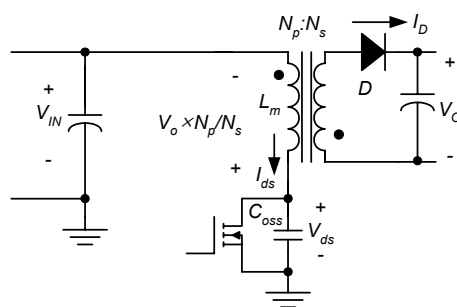

Figure 2. Typical Waveform of Quasi-Resonant Flyback Converter

3. Control Method of FSQ-Series

To overcome the frequency increase problem at light load, FSQ-series employs an advanced control technique illustrated in Figure 3 with typical switching waveforms. Once the MOSFET is turned on, the next turn-on is prohibited during the blanking time (t_B). After the blanking time, the controller finds the valley within the detection time window (t_W) and turns on the MOSFET (Case B and C). If no valley is found within t_W, the MOSFET is forced to turn on at the end of t_W (Case A). Thus, the converter can operate with a fixed frequency when operating in continuous conduction mode (CCM). Meanwhile, when the converter operates in discontinuous conduction mode (DCM), the controller turns on the MOSFET at the valley within t_W. Accordingly, the switching frequency is limited between 55kHz and 67kHz, as shown in Figure 3 and 4. This allows converter design as simple as in conventional PWM converters.
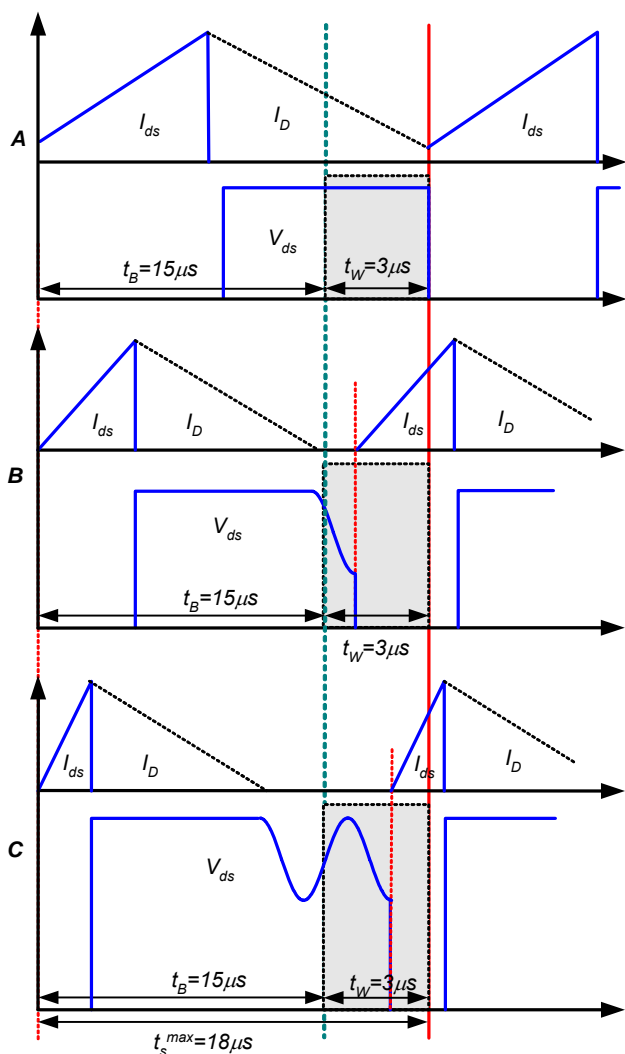
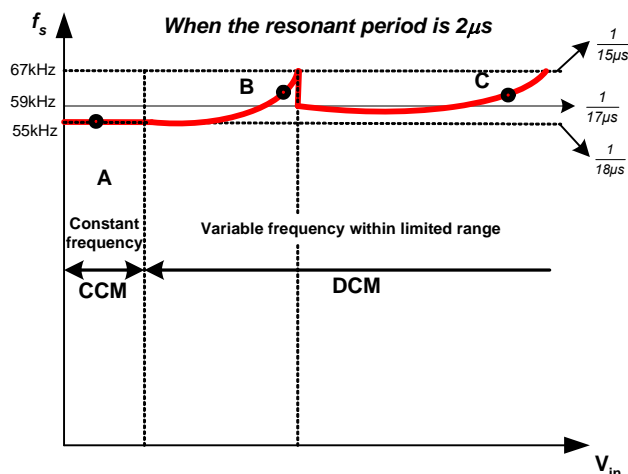**Figure 3. Switching Waveforms of FSQ-Series for Different Input Voltages**

Figure 4. Frequency Variation as Input Voltage Varies

4. Step-by-step Design Procedure

This section provides a step-by-step design process, illustrated in the design flow chart of the Figure 5. Figure 6 shows the basic schematic of quasi-resonant flyback converter using FSQ-series, which also serves as a reference circuit for the design process described.
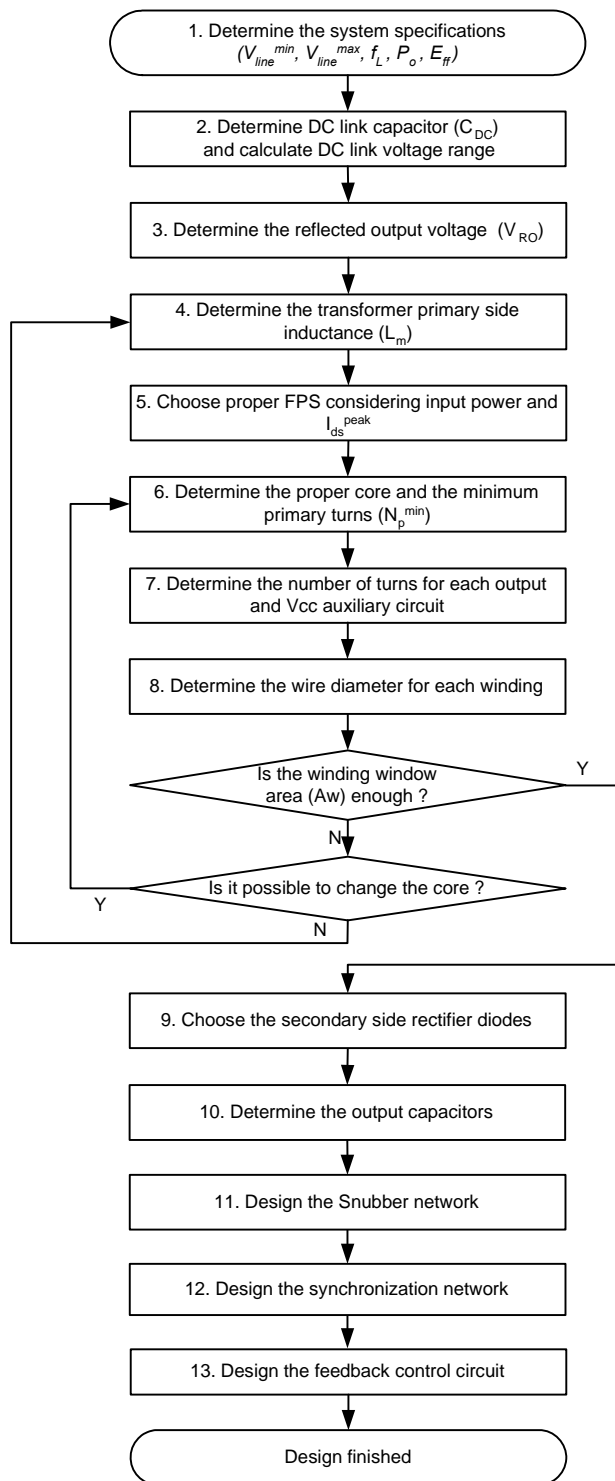

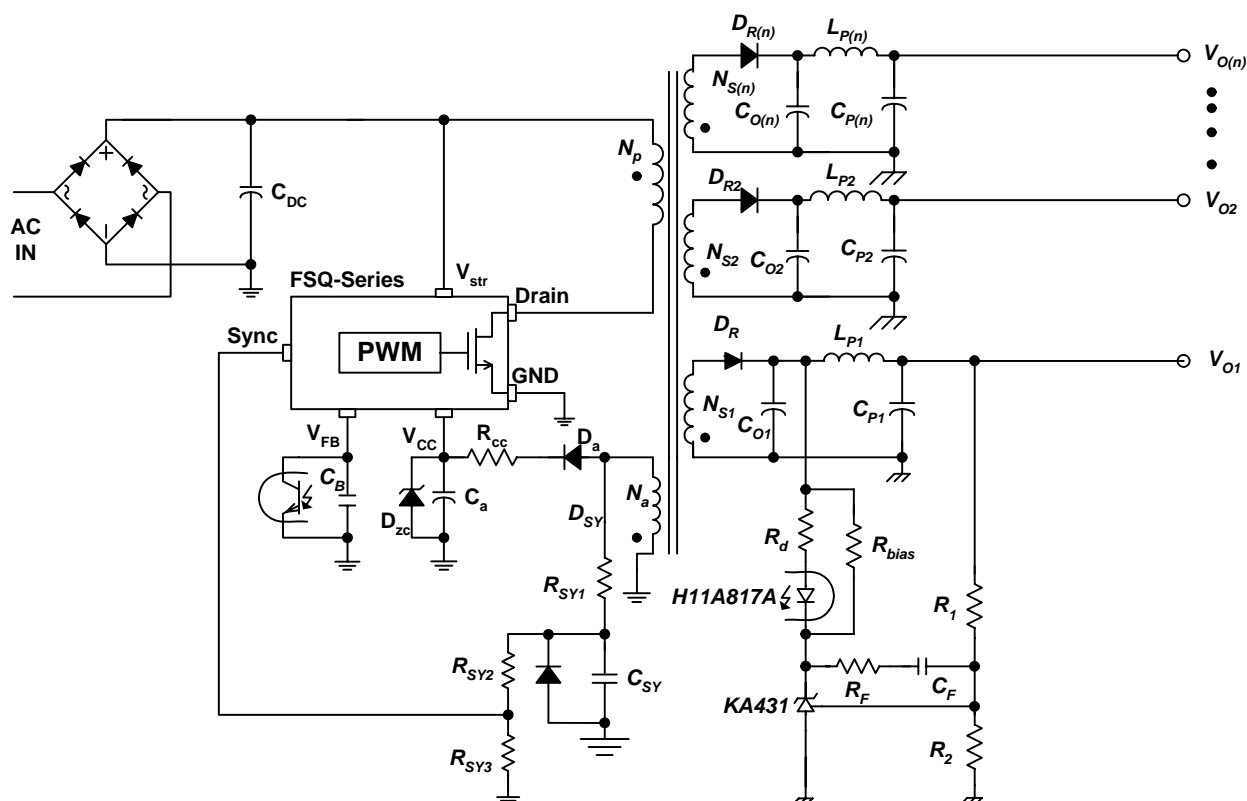**Figure 5. Flow Chart of Design Procedure**

Figure 6. Basic Quasi-Resonant Converter (QRC) Using FSQ-Series

[STEP-1] Define the System Specifications

When designing a power supply the following specifications should be determined first:

■ Line voltage range (V_{line}^{min} and V_{line}^{max}).
■ Line frequency (f_L).
■ Maximum output power (P_o).
■ Estimated efficiency (E_{ff}): The power conversion efficiency must be estimated to calculate the maximum input power. If no reference data is available, set E_{ff} = 0.7~0.75 for low-voltage output applications and E_{ff} = 0.8~0.85 for high-voltage output applications. With the estimated efficiency, the maximum input power is given by:

$$P_{in} = \frac{P_o}{E_{ff}} \qquad \text{(EQ 1)}$$

For multiple output SMPS, the load occupying factor for each output is defined as:

$$K_{L(n)} = \frac{P_{o(n)}}{P_o} \qquad \text{(EQ 2)}$$

where $P_{o(n)}$ is the maximum output power for the n-th output. For single output SMPS, $K_{L(1)}$=1. It is assumed that V_{o1} is the reference output that is regulated by the feedback control in normal operation, as shown in Figure 6.

[STEP-2] Determine DC Link Capacitor (C_{DC}) Value and Calculate the DC Link Voltage Range

In offline SMPS applications, a crude DC voltage (V_{DC}) is obtained first on the DC link capacitor (C_{DC}) by rectifying the AC mains. Then, the crude DC voltage is converted into pure DC outputs. Typically, the DC link capacitor is selected as 2-3μF per watt of input power for universal input range (85~265V_{rms}) and 1μF per watt of input power for European input range (195~265Vrms). With the DC link capacitor selected, the minimum DC link voltage is obtained as:

$$V_{DC}^{min} = \sqrt{2 \cdot (V_{line}^{min})^2 - \frac{P_{in} \cdot (1 - D_{ch})}{C_{DC} \cdot f_L}} \qquad \text{(EQ 3)}$$

where C_{DC} is the DC link capacitor value; D_{ch} is the duty cycle ratio for C_{DC} to be charged as defined in Figure 7, which is typically about 0.2; P_{in}, V_{line}^{min} and f_L are specified in STEP-1.

The maximum DC link voltage is given as:

$$V_{DC}^{max} = \sqrt{2} V_{line}^{max} \qquad \text{(EQ 4)}$$

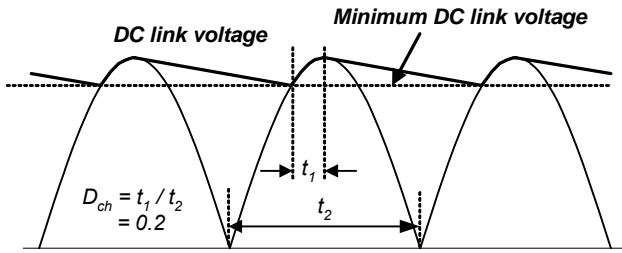where V_{line}^{max} is specified in STEP-1.

Figure 7. DC Link Voltage Waveform

[STEP-3] Determine the Reflected Output Voltage (V_{RO})

Figure 8 shows typical waveforms of the drain voltage of quasi-resonant flyback converter. When the MOSFET is turned off, the DC link voltage (V_{DC}), together with the output voltage reflected to the primary (V_{RO}), is imposed on the MOSFET. The maximum nominal voltage across the MOSFET (V_{ds}^{nom}) is:

$$V_{ds}^{nom} = V_{DC}^{max} + V_{RO} \qquad \text{(EQ 5)}$$

where V_{DC}^{max} is as specified in Equation 4. As shown in Figure 8, the capacitive switching loss of the MOSFET can be reduced by increasing V_{RO}. However, this increases the voltage stress on the MOSFET. Therefore, V_{RO} should be determined by a trade-off between the voltage margin of the MOSFET and the efficiency. It is typical to set V_{RO} as 60~90V so that V_{ds}^{norm} is 430~460V (65~70% of MOSFET rated voltage).
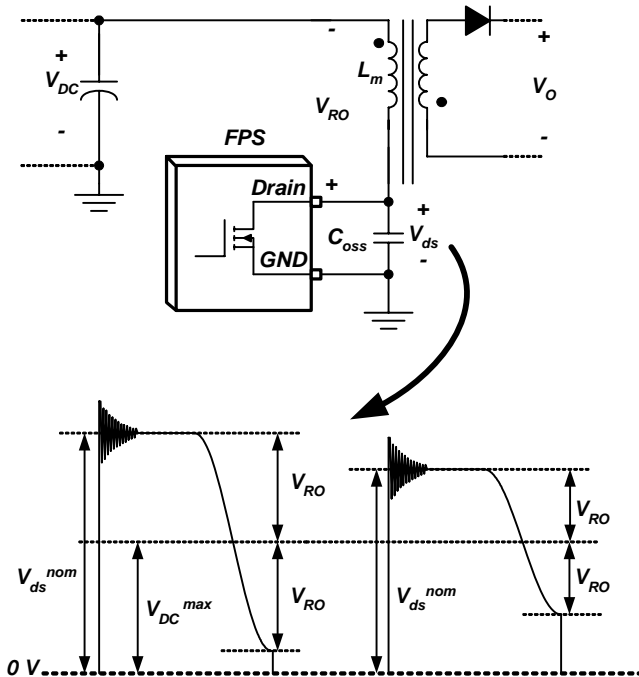

Figure 8. Typical Waveform of MOSFET Drain Voltage for Quasi-Resonant Converter

[STEP-4] Determine the Transformer Primary-Side Inductance (L_m)

The conventional quasi-resonant converter employs a variable frequency control, which makes the optimum design of the magnetic components difficult. However, FSQ-series can operate in both CCM and DCM with near constant switching frequency thanks to the advanced control technique, which allows engineers to use the conventional transformer design procedure of PWM converters.

In respect of EMI, DCM operation is preferred since the MOSFET is turned on at the minimum drain voltage and the secondary-side diode is softly turned off when operating in DCM. The transformer size can be reduced when using DCM because the average energy storage is low compared to CCM. However, DCM inherently causes higher RMS current, which increases the conduction loss of the MOSFET and the current stress on the output capacitors. When considering efficiency as well as magnetic components size, it is typical to design the converter to operate in CCM for low input voltage condition and in DCM for high input voltage condition.

The transformer primary side inductance is determined for the minimum input voltage and full-load condition. Once the reflected output voltage (V_{RO}) is determined in STEP-3, the flyback converter can be simplified, as shown in Figure 9, by neglecting the voltage drops in MOSFET and diode. The design rules are a bit different for CCM and DCM.

<u>CCM Design:</u> When designing a converter to operate in CCM at full load and minimum input voltage condition, the maximum duty ratio is given by:

$$D_{max} = \frac{V_{RO}}{V_{RO} + V_{DC}^{min}} \qquad \text{(EQ 6)}$$

where V_{DC}^{min} and V_{RO} are specified in Equation 3 and STEP-3, respectively.

With D_{max}, the primary-side inductance (L_m) of the transformer is obtained as:

$$L_m = \frac{(V_{DC}^{min} \cdot D_{max})^2}{2 P_{in} f_s K_{RF}} \qquad \text{(EQ 7)}$$

where V_{DC}^{min} is specified in Equation 3, P_{in} is specified in STEP-1, f_s is the free-running switching frequency of the FPS device, and K_{RF} is the ripple factor, shown in Figure 9. The ripple factor is closely related to the transformer size and the RMS value of the MOSFET current. It is typical to set $K_{RF} = 0.5$-0.7 for the universal input range.

<u>DCM Design:</u> When designing the converter to operate in DCM at full load and minimum input voltage condition, the maximum duty ratio should be chosen as smaller than the value obtained in Equation 6, as shown in Figure 9:

$$D_{max} < \frac{V_{RO}}{V_{RO} + V_{DC}^{min}} \qquad \text{(EQ 8)}$$

Since reducing D_{max} increases the conduction loss in

MOSFET, too small D_{max} should be avoided. Once D_{max} is determined, the primary-side inductance (L_m) of the transformer is obtained as:

$$L_m = \frac{(V_{DC}^{min} \cdot D_{max})^2}{2P_{in}f_s} \qquad \text{(EQ 9)}$$

where V_{DC}^{min} is specified in Equation 3, P_{in} is specified in STEP-1, and f_s is the free-running switching frequency of the FPS device.
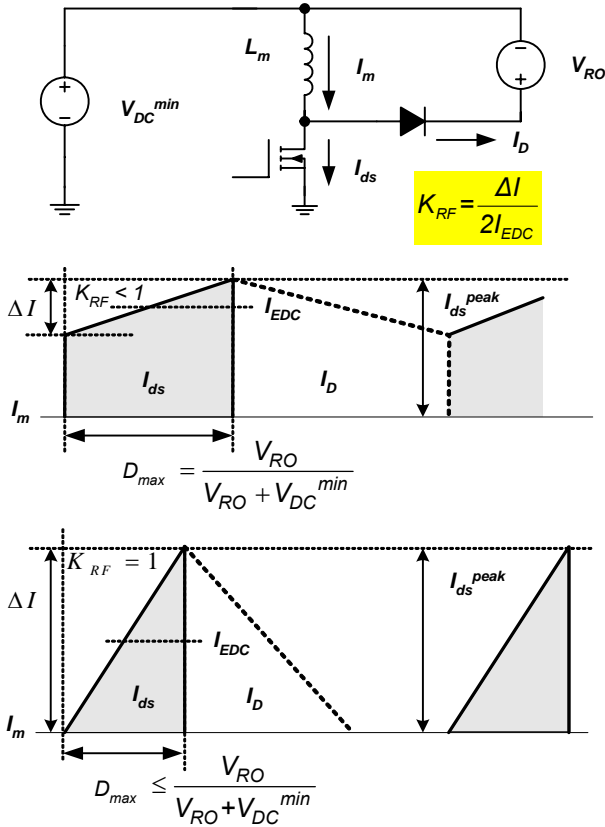

Figure 9. MOSFET Drain Current and Ripple Factor (K_{RF})

Once L_m is determined, the maximum peak current and RMS current of the MOSFET in minimum-input and full-load condition are obtained by:

$$I_{ds}^{peak} = I_{EDC} + \frac{\Delta I}{2} \qquad \text{(EQ 10)}$$

$$I_{ds}^{rms} = \sqrt{\left[3(I_{EDC})^2 + \left(\frac{\Delta I}{2}\right)^2\right]\frac{D_{max}}{3}} \qquad \text{(EQ 11)}$$

$$I_{EDC} = \frac{P_{in}}{V_{DC}^{min} \cdot D_{max}} \qquad \text{(EQ 12)}$$

$$\Delta I = \frac{V_{DC}^{min} D_{max}}{L_m f_s} \qquad \text{(EQ 13)}$$

where P_{in}, V_{DC}^{min}, D_{max}, and L_m are specified in Equations

1, 3, 6, and 7, respectively, and f_s is the FPS free-running switching frequency.

[STEP-5] Choose the Proper FPS Considering Input Power and Peak Drain Current

With the resulting maximum peak drain current of the MOSFET (I_{ds}^{peak}) from Equation 10, choose the proper FPS for which the pulse-by-pulse current limit level (I_{LIM}) is higher than I_{ds}^{peak}. Since FPS has $\pm$ 12% tolerance of I_{LIM}, there should be some margin in choosing the FPS device.

[STEP-6] Determine the Proper Core and the Minimum primary Turn

The initial selection of the core is bound to be crude since there are too many variables. One way to select the proper core is to refer to the manufacture's core selection guide. If there is no reference, use Table 1 as a starting point. The core recommended in Table 1 is typical for the universal input range, 55kHz switching frequency, and single-output application. When the input voltage range is 195-265 V_{AC} or the switching frequency is higher than 55kHz, a smaller core can be used. For an application with multiple outputs, a larger core than recommended in the table should usually be used.

With the chosen core, calculate the minimum number of turns for the transformer primary side to avoid the core saturation with the following:

$$N_P^{min} = \frac{L_m I_{LIM}}{B_{sat}A_e} \times 10^6 \quad \text{(turns)} \qquad \text{(EQ 14)}$$

where L_m is specified in Equation 7, I_{LIM} is the FPS pulse-by-pulse current limit level, A_e is the cross-sectional area of the core in mm^2, as shown in Figure 10, and B_{sat} is the saturation flux density in tesla. Figure 11 shows the typical characteristics of ferrite core from TDK (PC40). Since the saturation flux density (B_{sat}) decreases as the temperature goes high, the high temperature characteristics should be considered. $\pm$12% tolerance of I_{LIM} should be considered.

If there is no reference data, use B_{sat} =0.3~0.35 T. Since the MOSFET drain current exceeds I_{ds}^{peak} and reaches I_{LIM} in a transition or fault condition, I_{LIM} is used in Equation 14 instead of I_{ds}^{peak} to prevent core saturation during transition.
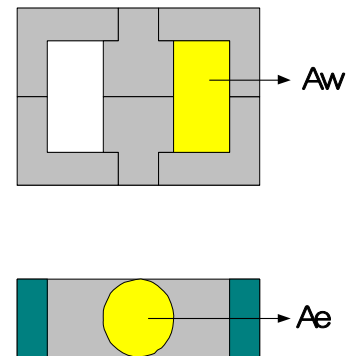

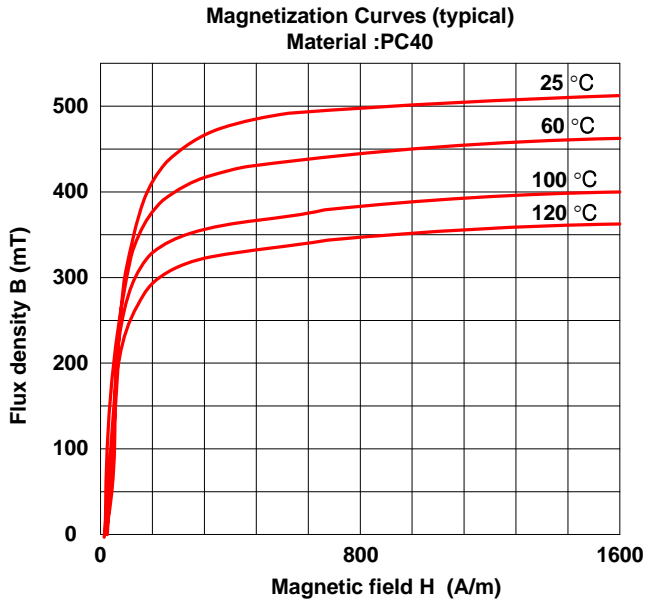**Figure 10. Window Area and Cross-Sectional Area**

Magnetization Curves (typical)
Material :PC40

**Figure 11. Typical B-H Characteristics of Ferrite Core
(TDK/PC40)**

Output Power	EI Core	EE Core	EPC Core	EER Core
0-10W	EI12.5 EI16 EI19	EE8 EE10 EE13 EE16	EPC10 EPC13 EPC17	
10-20W	EI22	EE19	EPC19	
20-30W	EI25	EE22	EPC25	EER25.5
30-50W	EI28 EI30	EE25	EPC30	EER28
50-70W	EI35	EE30		EER28L

**Table 1. Core Quick selection Table (for Universal Input
Range, fs=55kHz and Single Output)**

[STEP-7] Determine the Number of Turns for Each Output

Figure 12 shows the simplified diagram of the transformer. First, determine the turns ratio (n) between the primary side and the feedback-controlled secondary side as a reference.

$$n = \frac{N_P}{N_{s1}} = \frac{V_{RO}}{V_{o1} + V_{F1}} \qquad \text{(EQ 15)}$$

where N_p and N_{s1} are the number of turns for primary side and reference output, respectively, V_{o1} is the output voltage and V_{F1} is the diode (D_{R1}) forward voltage drop of the reference output.

Then, determine the proper integer for N_{s1} so that the

resulting N_p is larger than the $N_p{}^{min}$ obtained from Equation 14. The number of turns for the other output (n-th output) is determined by:

$$N_{s(n)} = \frac{V_{o(n)} + V_{F(n)}}{V_{o1} + V_{F1}} \cdot N_{s1} \qquad (turns) \quad \text{(EQ 16)}$$

The number of turns for V_{cc} winding is determined as:

$$N_a = \frac{V_{cc}{}^* + V_{Fa}}{V_{o1} + V_{F1}} \cdot N_{s1} \qquad (turns) \quad \text{(EQ 17)}$$

where $V_{cc}{}^*$ is the nominal value of the supply voltage of the FPS device and V_{Fa} is the forward voltage drop of D_a as defined in Figure 12. It is typical to set $V_{cc}{}^*$ 3~4V below V_{cc} maximum rating (refer to the datasheet).
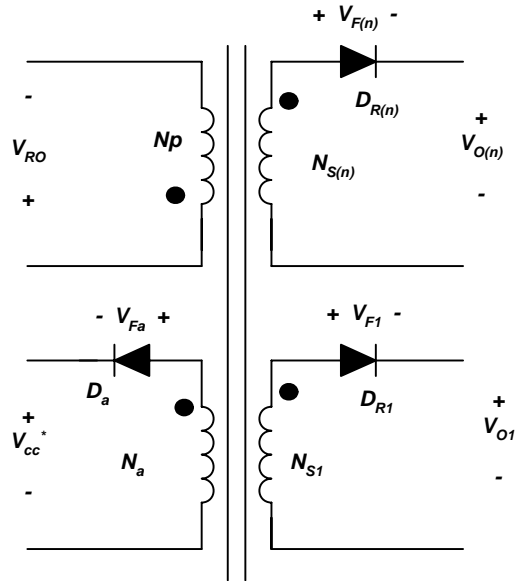

Figure 12. Simplified Diagram of the Transformer

With the determined turns of the primary side, the gap length of the core is obtained as:

$$G = 0.4 \times \pi A_e \left(\frac{N_P{}^2}{10^9 L_m} - \frac{1}{A_L} \right) \qquad (mm) \quad \text{(EQ 18)}$$

where A_L is the AL-value with no gap in nH/turns[2]; A_e is the cross-sectional area of the core in mm[2], as shown in Figure 10; L_m is specified in Equation 7; and N_p is the number of turns for the primary-side of the transformer.

[STEP-8] Determine the Wire Diameter for Each Winding Based on the rms Current of Each Output

The rms current of the n-th secondary winding is obtained as:

$$I_{sec(n)}{}^{rms} = I_{ds}{}^{rms} \sqrt{\frac{1 - D_{max}}{D_{max}} \cdot \frac{V_{RO} \cdot K_{L(n)}}{(V_{o(n)} + V_{F(n)})}} \qquad \text{(EQ 19)}$$

where V_{RO} and $I_{ds}{}^{rms}$ are specified in STEP-3 and Equation 11, respectively; $V_o(n)$ is the output voltage of the n-th output; $V_{F(n)}$ is the diode ($D_{R(n)}$) forward voltage drop; D_{max} is specified in Equation 6; and $K_{L(n)}$ is the load-occupying factor for n-th output defined in Equation 2.

The current density is typically 5A/mm^2 when the wire is greater than 1m long. When the wire is short, with a small number of turns, a current density of 6-10 A/mm^2 is also acceptable. Avoid using wire with a diameter larger than 1mm to avoid severe eddy current losses and to make winding easier.

For high current output, it is better to use parallel windings with multiple strands of thinner wire to minimize skin effect.

Verify that if the winding window area of the core, A_w is enough to accommodate the wires (refer to Figure 10). The required winding window area (A_{wr}) is given by:

$$A_{wr} = A_c / K_F \qquad \text{(EQ 20)}$$

where A_c is the actual conductor area and K_F is the fill factor. Typically the fill factor is 0.2~0.25 for single-output application and 0.15~0.2 for multiple outputs application.

If the required window (A_{wr}) is larger than the actual window area (A_w), go back to STEP-6 and increase the core. If it is impossible to change the core due to cost or size constraints and the converter is designed for CCM and the winding window (A_w) is slightly insufficient, go back to STEP-4 and reduce L_m by increasing the ripple factor (K_{RF}). The minimum number of turns for the primary ($N_p{}^{min}$) of Equation 14 decreases, which results in the reduced required winding window area (A_{wr}).

[STEP-9] Choose the Rectifier Diode in the Secondary Side Based on the Voltage and Current Ratings.

The maximum reverse voltage and the rms current of the rectifier diode ($D_{R(n)}$) of the n-th output are obtained as:

$$V_{D(n)} = V_{o(n)} + \frac{V_{DC}{}^{max} \cdot (V_{o(n)} + V_{F(n)})}{V_{RO}} \qquad \text{(EQ 21)}$$

$$I_{D(n)}{}^{rms} = I_{ds}{}^{rms} \sqrt{\frac{V_{DC}{}^{min}}{V_{RO}} \cdot \frac{V_{RO} K_{L(n)}}{(V_{o(n)} + V_{F(n)})}} \qquad \text{(EQ 22)}$$

where $K_{L(n)}$, $V_{DC}{}^{max}$, V_{RO}, and $I_{ds}{}^{rms}$ are specified in Equations 2, 4, STEP-3 and Equation 11, respectively; D_{max} is specified in Equation 6; $V_{o(n)}$ is the output voltage of the n-th output; and $V_{F(n)}$ is the diode ($D_{R(n)}$) forward voltage. The typical voltage and current margins for the rectifier diode are:

$$V_{RRM} > 1.3 \cdot V_{D(n)} \qquad \text{(EQ 23)}$$

$$I_F > 1.5 \cdot I_{D(n)}{}^{rms} \qquad \text{(EQ 24)}$$

where V_{RRM} is the maximum reverse voltage and I_F is the average forward current of the diode.

[STEP-10] Determine the Output Capacitor Considering the Voltage and Current Ripple

The ripple current of the n-th output capacitor ($C_{o(n)}$) is obtained as:

$$I_{cap(n)}{}^{rms} = \sqrt{(I_{D(n)}{}^{rms})^2 - I_{o(n)}{}^2} \qquad \text{(EQ 25)}$$

where $I_{o(n)}$ is the load current of the n-th output and $I_{D(n)}{}^{rms}$ is specified in Equation 22. The ripple current should be smaller than the ripple current specification of the capacitor. The voltage ripple on the n-th output is given by:

$$\Delta V_{o(n)} = \frac{I_{o(n)} D_{max}}{C_{o(n)} f_s} + \frac{I_{ds}{}^{peak} V_{RO} R_{C(n)} K_{L(n)}}{(V_{o(n)} + V_{F(n)})} \qquad \text{(EQ 26)}$$

where $C_{o(n)}$ is the capacitance; $R_{c(n)}$ is the effective series resistance (ESR) of the n-th output capacitor; $K_{L(n)}$, V_{RO}, and $I_{ds}{}^{peak}$ are specified in Equation 2, STEP-3, and Equation 10, respectively; D_{max} is specified in Equation 6; $I_{o(n)}$ and $V_{o(n)}$ are the load current and output voltage of the n-th output, respectively; and $V_{F(n)}$ is the diode ($D_{R(n)}$) forward voltage.

If it is impossible to meet the ripple specification with a single output capacitor due to the high ESR of the electrolytic capacitor, additional LC filter stages (post filter) can be used. When using the post filters, be careful not to place the corner frequency too low. Too low a corner frequency may make the system unstable or limit the control bandwidth. It is typical to set the corner frequency of the post filter at around 10-20% of the switching frequency.

[STEP-11] Design the RCD Snubber

When the power MOSFET is turned off, there is a high voltage spike on the drain due to the transformer leakage inductance. This excessive voltage on the MOSFET may lead to an avalanche breakdown and, eventually, failure of the FPS. Therefore, it is necessary to use an additional network to clamp the voltage.

The RCD snubber circuit and MOSFET drain voltage waveform are shown in Figures 13 and 14, respectively. The RCD snubber network absorbs the current in the leakage inductance by turning on the snubber diode (D_{sn}) once the MOSFET drain voltage exceeds the voltage of node X, as depicted in Figure 13. In the analysis of snubber network, it is assumed that the snubber capacitor is large enough that its voltage does not change significantly during one switching cycle. The capacitor used in the snubber should be ceramic or a material that offers low ESR. Electrolytic or tantalum capacitors are unacceptable for these reasons.
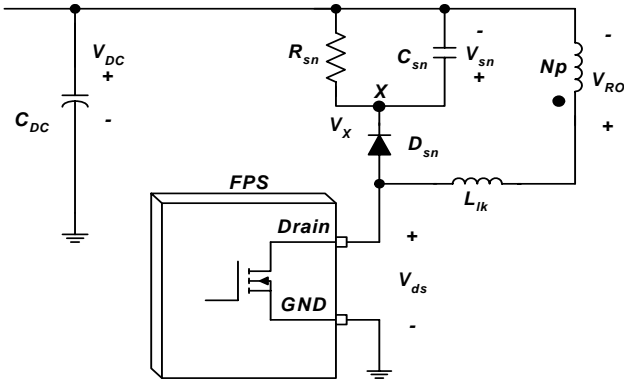
Figure 13. Circuit Diagram of the Snubber Network

The first step in designing the snubber circuit is to determine the snubber capacitor voltage (V_{sn}) at the minimum input voltage and full-load condition. Once V_{sn} is determined, the power dissipated in the snubber network at the minimum input voltage and full-load condition is obtained as:

$$P_{sn} = \frac{(V_{sn})^2}{R_{sn}} = \frac{1}{2}f_s L_{lk}(I_{ds}^{peak})^2 \frac{V_{sn}}{V_{sn} - V_{RO}} \qquad \text{(EQ 27)}$$

where I_{ds}^{peak} is specified in Equation 10, f_s is the FPS free-running switching frequency, L_{lk} is the leakage inductance, V_{sn} is the snubber capacitor voltage at the minimum input voltage and full-load condition, V_{RO} is the reflected output voltage, and R_{sn} is the snubber resistor. V_{sn} should be larger than V_{RO} and it is typical to set V_{sn} to be 2~2.5 times V_{RO}. Too small a V_{sn} results in a severe loss in the snubber network, as shown in Equation 27. The leakage inductance is measured at the switching frequency on the primary winding with all other windings shorted.

The snubber resistor with proper rated wattage should be chosen based on the power loss. The maximum ripple of the snubber capacitor voltage is obtained as:

$$\Delta V_{sn} = \frac{V_{sn}}{C_{sn} R_{sn} f_s} \qquad \text{(EQ 28)}$$

where f_s is the FPS free-running switching frequency. In general, 5~10% ripple of the selected capacitor voltage is

reasonable.

The snubber capacitor voltage (V_{sn}) of Equation 27 is for the minimum input voltage and full-load condition. When the converter is designed to operate in CCM under this condition, the peak drain current, together with the snubber capacitor voltage, decrease as the input voltage increases, as shown in Figure 14. The peak drain current at the maximum input voltage and full load condition (I_{ds2}^{peak}) is obtained as

$$I_{ds2}^{peak} = \sqrt{\frac{2 \cdot P_{in}}{f_s \cdot L_m}} \qquad \text{(EQ 29)}$$

where P_{in}, and L_m are specified in Equations 1 and 7, respectively, and f_s is the FPS free-running switching frequency.

The snubber capacitor voltage under maximum input voltage and full load condition is obtained as:

$$V_{sn2} = \frac{V_{RO} + \sqrt{(V_{RO})^2 + 2R_{sn}L_{lk}f_s(I_{ds2}^{peak})^2}}{2} \qquad \text{(EQ 30)}$$

where f_s is the FPS free-running switching frequency, L_{lk} is the primary-side leakage inductance, V_{RO} is the reflected output voltage, and R_{sn} is the snubber resistor.
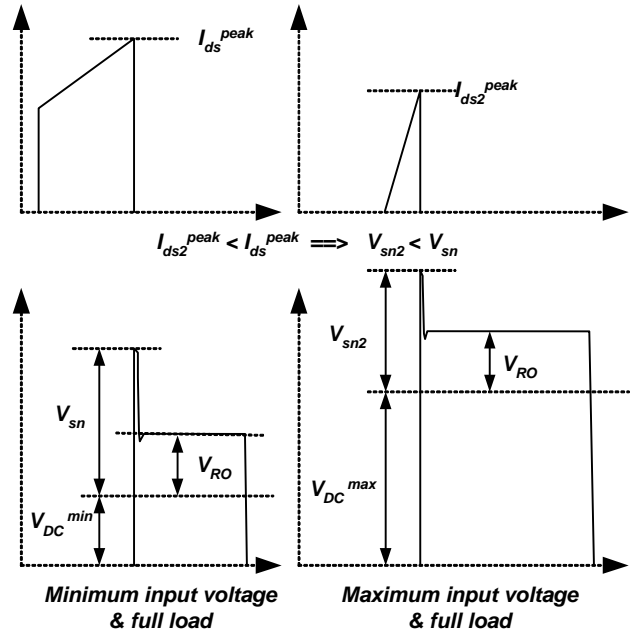

Figure 14. MOSFET Drain Voltage and Snubber Capacitor Voltage

From Equation 30, the maximum voltage stress on the internal MOSFET is given by:

$$V_{ds}^{max} = V_{DC}^{max} + V_{sn2} \qquad \text{(EQ 31)}$$

where V_{DC}^{max} is specified in Equation 4.

Verify that V_{ds}^{max} is below 90% of the rated voltage of the MOSFET (*BVdss*), as shown in Figure 15. The voltage rating of the snubber diode should be higher than *BVdss*. Usually, an ultra fast diode with 1A current rating is used for the snubber network.

In the snubber design in this section, neither the lossy discharge of the inductor, nor stray capacitance, is considered. In the actual converter, the loss in the snubber network is generally less than the designed value.
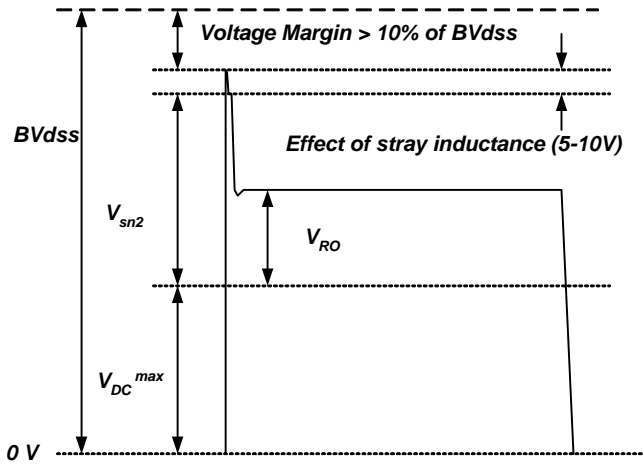

Figure 15. MOSFET Drain Voltage and Snubber Capacitor Voltage

[STEP-12] Design the Synchronization Network

The optimum MOSFET turn-on point is indirectly detected by monitoring the V_{cc} winding voltage, as shown in Figures 16 and 17. The output of the sync-detect comparator (CO) becomes high when the sync voltage (V_{sync}) rises above 0.7V and becomes low when the V_{sync} drops below 0.2V. The MOSFET is turned on at the falling edge of the sync-detect comparator output (CO).

To synchronize the V_{sync} with the MOSFET drain voltage, the sync capacitor (C_{SY}) should be chosen so that T_Q is same as a quarter of the resonance period ($T_R/4$), as shown in Figure 17. $T_R/4$ and T_Q are given as:

$$\frac{T_R}{4} = \frac{\pi \cdot \sqrt{L_m \cdot C_{eo}}}{2} \qquad \text{(EQ 32)}$$

$$T_Q = \frac{R_{SY1} \cdot (R_{SY2} + R_{SY3})}{R_{SY1} + R_{SY2} + R_{SY3}} \cdot C_{SY} + 200ns \qquad \text{(EQ 33)}$$

where L_m is the primary-side inductance of the transformer, C_{eo} is the effective MOSFET output capacitance, and 200ns is the internal delay time.
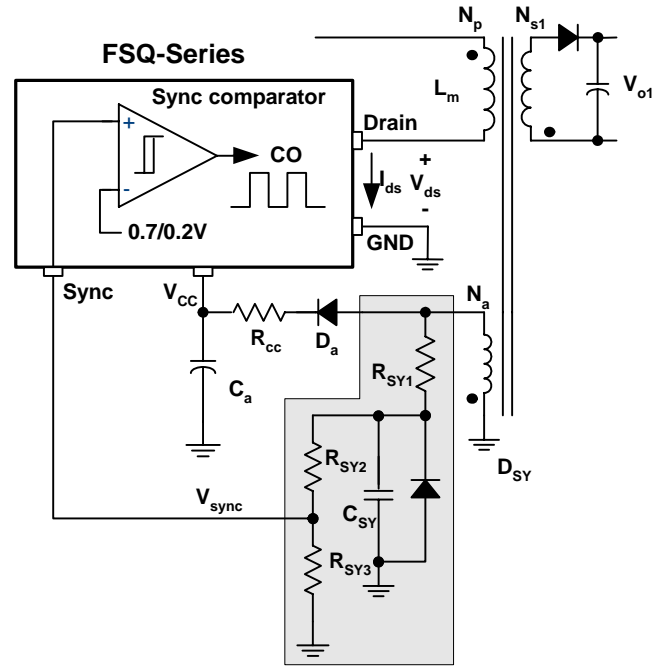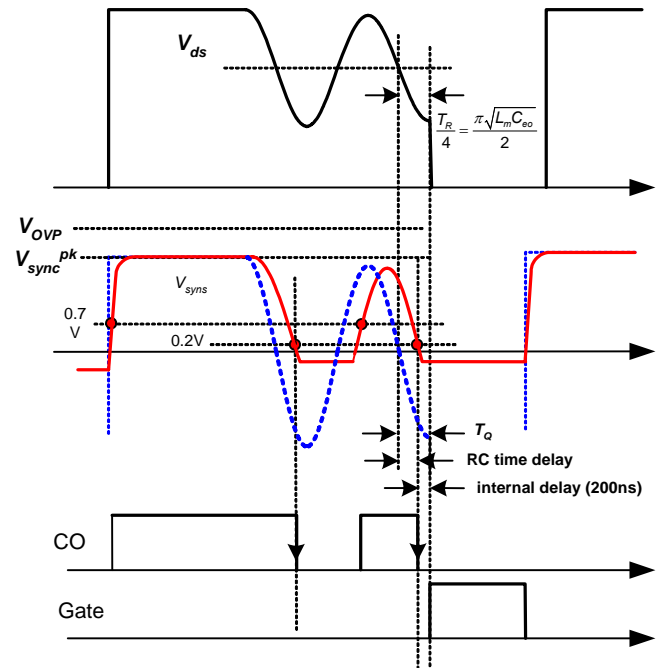

Figure. 16 Synchronization Circuit

Figure. 17 Synchronization Waveforms

The peak value of the sync signal is determined by the voltage divider network R_{SY1}, R_{SY2}, and R_{SY3} as

$$V_{sync}^{pk} = \frac{R_{SY3}}{R_{SY1} + R_{SY2} + R_{SY3}} \cdot \frac{N_a}{N_{S1}} \cdot (V_{01} + V_{F1}) \qquad \text{(EQ 34)}$$

where N_a and N_{s1} are the numbers of the turns for V_{cc} winding and V_{o1}, respectively, and V_{F1} is the forward voltage drop of D_1.

Choose the voltage divider R_{SY1}, R_{SY2}, and R_{SY3} so that the peak value of sync voltage ($V_{sync}{}^{pk}$) is lower than the OVP threshold voltage (6V) to avoid triggering OVP in normal operation. It is typical to set $V_{sync}{}^{pk}$ to be 4~5V.

[STEP-13] Design the Feedback Loop

Since FSQ-series employs current-mode control, the feedback loop can be simply implemented with a one-pole and one-zero compensation circuit, as shown in Figure 18. In the feedback circuit analysis, it is assumed that the current transfer ratio (CTR) of the opto-coupler is 100%.

The current control factor of FPS, K is defined as:

$$K = \frac{I_{pk}}{V_{FB}} = \frac{I_{LIM}}{V_{FBsat}} \qquad \text{(EQ 35)}$$

where I_{pk} is the peak drain current and V_{FB} is the feedback voltage, respectively, for a given operating condition; I_{LIM} is the current limit of the FPS; and V_{FBsat} is the feedback saturation voltage, which is typically 2.5V.

To express the small signal AC transfer functions, the small signal variations of feedback voltage (v_{FB}) and controlled output voltage (v_{o1}) are introduced as $\hat{v}_{FB}$ and $\hat{v}_{o1}$.
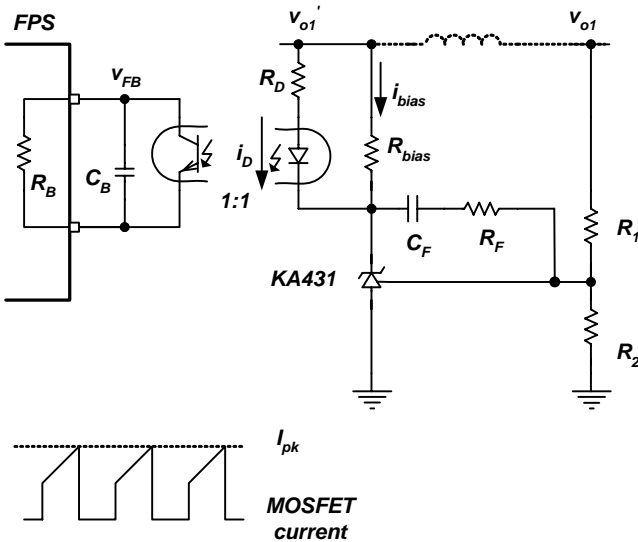

Figure 18. Control Block Diagram

For CCM operation, the control-to-output transfer function of the flyback converter, using current-mode control, is given by:

$$G_{vc} = \frac{\hat{v}_{o1}}{\hat{v}_{FB}} \qquad \text{(EQ 36)}$$

$$= \frac{K \cdot R_L V_{DC}(N_p / N_{s1})}{2V_{RO} + V_{DC}} \cdot \frac{(1 + s/w_z)(1 - s/w_{rz})}{1 + s/w_p}$$

where V_{DC} is the DC input voltage; R_L is the effective total load resistance of the controlled output, defined as $V_{o1}{}^2/P_o$; N_p and N_{s1} are specified in STEP-7; V_{RO} is specified in STEP-3; V_{o1} is the reference output voltage; P_o is specified in STEP-1; and K is specified in Equation 35. The pole and zeros of Equation 36 are defined as:

$$w_z = \frac{1}{R_{c1}C_{o1}}, \; w_{rz} = \frac{R_L(1-D)^2}{DL_m(N_{s1}/N_p)^2} \; and \; w_p = \frac{(1+D)}{R_L C_{o1}}$$

$$\text{(EQ 37)}$$

where L_m is specified in Equation 7, D is the duty cycle of the FPS, C_{o1} is the reference output capacitor, and R_{C1} is the ESR of C_{o1}.

When the converter has more than one output, the low frequency control-to-output transfer function is proportional to the parallel combination of all load resistance, adjusted by the square of the turns ratio. Therefore, the effective load resistance is used in Equation 36 instead of the actual load resistance of V_{o1}.

Notice that there is a right half plane (RHP) zero (w_{rz}) in the control-to-output transfer function of Equation 36. Because the RHP zero reduces the phase by 90°, the crossover frequency should be placed below the RHP zero.

Figure 19 shows the variation of a CCM flyback converter control-to-output transfer function for different input voltages. This figure shows the system poles and zeros, together with the DC gain change, for different input voltages. The gain is highest at the high input voltage condition and the RHP zero is lowest at the low input voltage condition.

Figure 20 shows the variation of a CCM flyback converter control-to-output transfer function for different loads. This figure shows that the low frequency gain does not change for different loads and the RHP zero is lowest at the full-load condition.

For DCM operation, the control-to-output transfer function of the flyback converter, using current-mode control, is given by:

$$G_{vc} = \frac{\hat{v}_{o1}}{\hat{v}_{FB}} = \frac{V_{o1}}{V_{FB}} \cdot \frac{(1 + s/w_z)}{(1 + s/w_p)} \qquad \text{(EQ 38)}$$

$$where \quad w_z = \frac{1}{R_{c1}C_{o1}} \; , \; w_p = 2/R_L C_{o1},$$

V_{o1} is the reference output voltage, V_{FB} is the feedback voltage for a given condition, R_L is the effective total

resistance of the controlled output, C_{o1} is the controlled output capacitance, and R_{c1} is the ESR of C_{o1}.

Figure 21 shows the variation of the control-to-output transfer function of a flyback converter in DCM for different loads. Contrary to the flyback converter in CCM, there is no RHP zero and the DC gain does not change as the input voltage varies. As can be seen, the overall gain, except for the DC gain, is highest at the full-load condition.

The feedback compensation network transfer function of Figure 18 is obtained as:

$$\frac{\hat{v}_{FB}}{\hat{v}_{o1}} = -\frac{w_i}{s} \cdot \frac{1 + s/w_{zc}}{1 + 1/w_{pc}} \qquad \text{(EQ 39)}$$

$$where \; w_i \; = \frac{R_B}{R_1 R_D C_F} ; w_{zc} = \frac{1}{(R_F + R_1)C_F} ; \; w_{pc} = \frac{1}{R_B C_B};$$

R_B is the internal feedback bias resistor of FPS, which is typically 2.8kΩ; and R_1, R_D, R_F, C_F and C_B are shown in Figure 18.
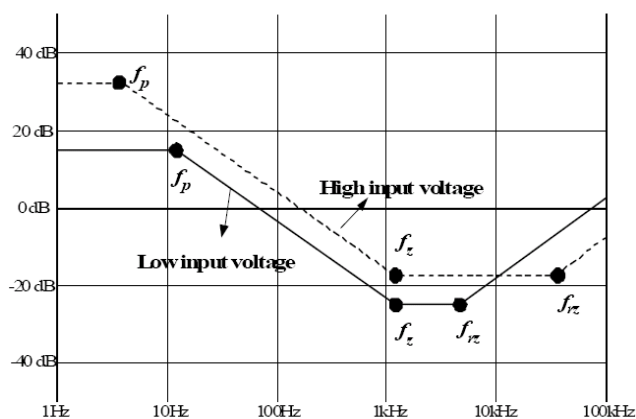

Figure 19. CCM Flyback Converter Control-to-Output Transfer Function Variation for Different Input Voltages
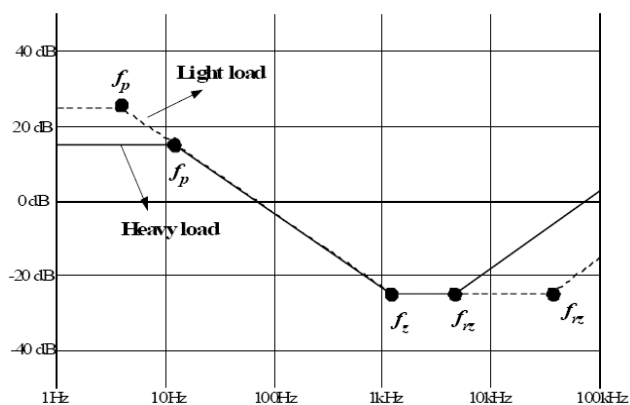

Figure 20. CCM Flyback Converter Control-to-Output Transfer Function Variation for Different Loads
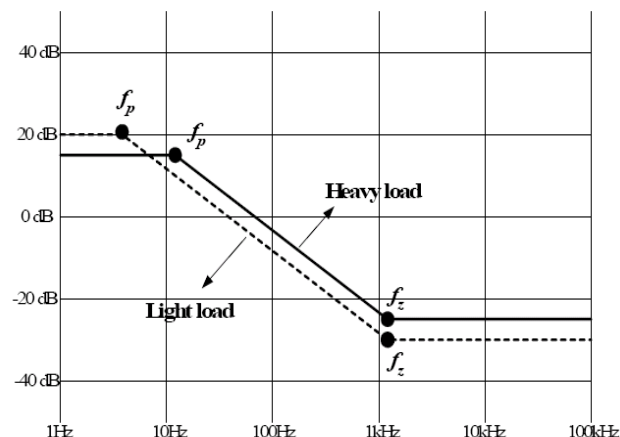

Figure 21. DCM Flyback Converter Control-to-Output TransferFunction Variation for Different Loads

When the input voltage and the load current vary over a wide range, it is not easy to determine the worst case for the feedback-loop design. The gain, together with zeros and poles, varies according to the operating condition. Even though the converter is designed to operate in CCM or at the boundary of DCM and CCM in the minimum input voltage and full-load condition, the converter enters into DCM, changing the system transfer functions as the load current decreases and/or input voltage increases.

One simple and practical solution to this problem is designing the feedback loop for low input voltage and full-load condition with enough phase and gain margin. When the converter operates in CCM, the RHP zero is lowest in low input voltage and full-load condition. The gain increases about 6dB as the operating condition is changed from the lowest input voltage to the highest input voltage condition under universal input condition. When the operating mode changes from CCM to DCM, the RHP zero disappears, making the system stable. Therefore, by designing the feedback loop with more than 45° of phase margin in low input voltage and full load condition, the stability over the operating ranges can be guaranteed.

The procedure to design the feedback loop is as follows:

■ Determine the crossover frequency (f_c). For CCM mode flyback, set f_c below 1/3 of right half plane (RHP) zero to minimize the effect of the RHP zero. For DCM mode, f_c can be placed at a higher frequency, since there is no RHP zero.

■ When an additional LC filter is employed, the crossover frequency should be placed below 1/3 of the corner frequency of the LC filter, since it introduces a -180° phase drop. Never place the crossover frequency beyond the corner frequency of the LC filter. If the crossover

frequency is too close to the corner frequency, the controller should be designed to have a phase margin greater than 90° when ignoring the effect of the post filter.

■ Determine the DC gain of the compensator (w_i/w_{zc}) to cancel the control-to-output gain at f_c.

■ Place a compensator zero (f_{zc}) around $f_c/3$.
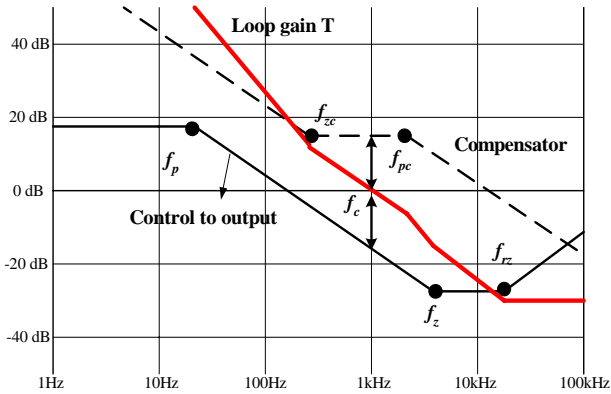
■ Place a compensator pole (f_{pc}) above $3f_c$.

Figure 22. Compensator design

Determining the feedback circuit component includes some restrictions, such as:

■ The voltage divider network of R_1 and R_2 should be designed to provide 2.5V to the reference pin of the KA431. The relationship between R_1 and R_2 is given as:

$$R_2 = \frac{2.5 \cdot R_1}{V_{o1} - 2.5} \qquad \text{(EQ 40)}$$

where V_{o1} is the reference output voltage.

■ The capacitor connected to feedback pin (C_B) is related to the shutdown delay time in an overload condition by:

$$t_{delay} = (V_{SD} - 2.5) \cdot C_B / I_{delay} \qquad \text{(EQ 41)}$$

where V_{SD} is the shutdown feedback voltage and I_{delay} is the shutdown delay current. These values are given in the product datasheet. A 10 ~ 50ms delay time is typical for most applications. Because C_B also determines the high-frequency pole (w_{pc}) of the compensator transfer function, as shown in Equation 39, too large a C_B can limit the control bandwidth by placing w_{pc} at too low a frequency. A typical value for C_B is 10-50nF.

■ The resistors R_{bias} and R_D, used together with opto-coupler H11A817A and shunt regulator KA431, should be designed to provide proper operating current for the KA431 and to guarantee the full swing of the feedback voltage for the FPS device chosen. In general, the minimum cathode voltage and current for the KA431 are 2.5V and 1mA, respectively. Therefore, R_{bias} and R_D should be designed to satisfy the following conditions:

$$\frac{V_{o1} - V_{OP} - 2.5}{R_D} > I_{FB} \qquad \text{(EQ 42)}$$

$$\frac{V_{OP}}{R_{bias}} > 1mA \qquad \text{(EQ 43)}$$

where V_{o1} is the reference output voltage; V_{OP} is opto-diode forward voltage drop, which is typically 1V; and I_{FB} is the feedback current of FPS, which is typically 1mA. For example, $R_{bias} < 1k\Omega$ and $R_D < 1.5k\Omega$ for V_{o1}=5V.

Miscellaneous Notes

■ V_{cc} capacitor (C_a): The typical value for C_a is 10-50µF, which is enough for most applications. A smaller capacitor than this may result in an under-voltage lockout of FPS during the startup. Too large a capacitor may increase the start-up time.

■ V_{cc} resistor (R_a): The typical value for R_a is 5-20Ω. In the case of multiple outputs flyback converter, the voltage of the lightly loaded output, such as V_{cc}, varies as the load currents of other outputs change due to the imperfect coupling of the transformer. R_a reduces the sensitivity of V_{cc} to other outputs and improves the regulations of V_{cc}.

Design Example

Application	Device	Input Voltage	Output Power	Output Voltage (Rated Current)
DVD player	FSQ0365RN	85-265VAC (60Hz)	18.1W	5.1V (1.0A)
				3.4V (1.0A)
				12V (0.4A)
				16V (0.3A)

Key Design Notes

To maximize the efficiency, the power supply is designed to operate in CCM for minimum input-voltage and full-load condition and in DCM for high input voltage condition.

1. Schematic

2. Transformer Specifications
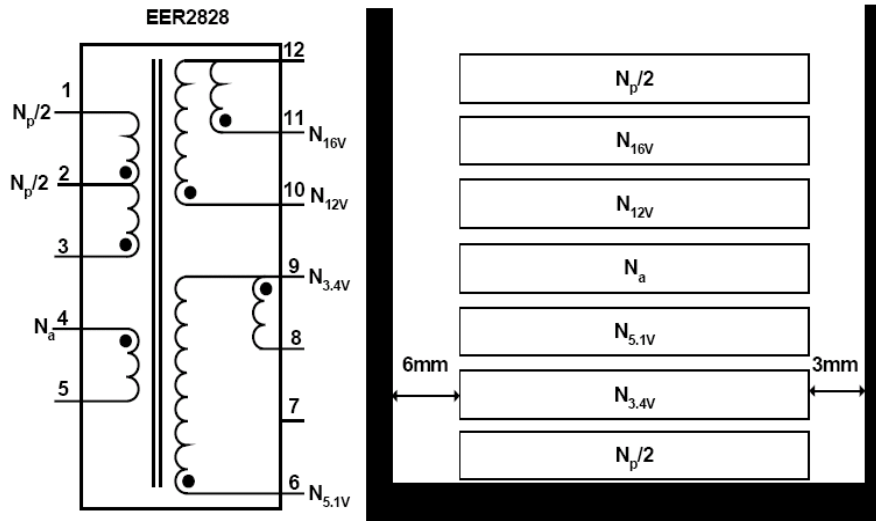
No	Pin (s→f)	Wire	Turns	Winding Method
$N_p/2$	3 → 2	$0.25^\phi \times 1$	50	Center Solenoid Winding
Insulation: Polyester Tape t = 0.050mm, 2 Layers				
$N_{3.4V}$	9 → 8	$0.33^\phi \times 2$	4	Center Solenoid Winding
Insulation: Polyester Tape t = 0.050mm, 2 Layers				
N_{5V}	6 → 9	$0.33^\phi \times 1$	2	Center Solenoid Winding
Insulation: Polyester Tape t = 0.050mm, 2 Layers				
N_a	4 → 5	$0.25^\phi \times 1$	16	Center Solenoid Winding
Insulation: Polyester Tape t = 0.050mm, 2 Layers				
N_{12V}	10 → 12	$0.33^\phi \times 3$	14	Center Solenoid Winding
Insulation: Polyester Tape t = 0.050mm, 3 Layers				
N_{16V}	11 → 12	$0.33^\phi \times 3$	18	Center Solenoid Winding
Insulation: Polyester Tape t = 0.050mm, 2 Layers				
$N_p/2$	2 → 1	$0.25^\phi \times 1$	50	Center Solenoid Winding
Insulation: Polyester Tape t = 0.050mm, 2 Layers				

Core: EER2828 (Ae=86.7mm^2)

Bobbin: EER2828

Electrical Characteristics

	Pin	Specification	Remarks
Inductance	1 - 3	1.4mH ± 10%	100kHz, 1V
Leakage	1 - 3	25µH Max	Short all other pins

Hang-Seok Choi, Ph.D.

Power Conversion / Fairchild Semiconductor
Phone: +82-32-680-1383 Facsimile : +82-32-680-1317
Email: hangseok.choi@fairchildsemi.com